Orientation tuning of contrast masking caused by motion streaks

Deborah Apthorp School of Psychology, University of Sydney, Sydney, Australia

John Cass School of Psychology, University of Western Sydney, Sydney, Australia, & MARCS Auditory Research Laboratories, University of Western Sydney, Milperra, Australia

David Alais School of Psychology, University of Sydney, Sydney, Australia

We investigated whether the oriented trails of blur left by fast-moving dots (i.e., "motion streaks") effectively mask grating targets. Using a classic overlay masking paradigm, we varied mask contrast and target orientation to reveal underlying tuning. Fast-moving Gaussian blob arrays elevated thresholds for detection of static gratings, both monoptically and dichoptically. Monoptic masking at high mask (i.e., streak) contrasts is tuned for orientation and exhibits a similar bandwidth to masking functions obtained with grating stimuli (~30 degrees). Dichoptic masking fails to show reliable orientation-tuned masking, but dichoptic masks at very low contrast produce a narrowly tuned facilitation (~17 degrees). For iso-oriented streak masks and grating targets, we also explored masking as a function of mask contrast. Interestingly, dichoptic masking shows a classic "dipper"-like TVC function, whereas monoptic masking shows no dip and a steeper "handle". There is a very strong unoriented component to the masking, which we attribute to transiently biased temporal frequency masking. Fourier analysis of "motion streak" images shows interesting differences between dichoptic and monoptic functions and the information in the stimulus. Our data add weight to the growing body of evidence that the oriented blur of motion streaks contributes to the processing of fast motion signals.

Keywords: motion—2D, binocular vision, masking, temporal vision

Citation: Apthorp, D., Cass, J., & Alais, D. (2010). Orientation tuning of contrast masking caused by motion streaks. *Journal of Vision, 10*(10):11, 1–13, http://www.journalofvision.org/content/10/10/11, doi:10.1167/10.10.11.

Introduction

Many models addressing the visual system's spatiotemporal decomposition of motion stimuli assume a classical energy filter model in which motion-sensitive units are optimally stimulated by motion that is orthogonal to their preferred orientation (Adelson & Bergen, 1985; Carandini, Heeger, & Movshon, 1997; De Valois, Yund, & Hepler, 1982; van Santen & Sperling, 1985; Watson & Ahumada, 1985). Recently, however, it been suggested that another spatiotemporal aspect of motion—the static, oriented smear or "motion streak" left by a fast-moving stimulus—might act in combination with cortical motion signals to determine direction of motion (Geisler, 1999). Using one-dimensional dynamic noise to mask the motion of a translating Gaussian blob, Geisler found increased luminance detection thresholds for the blob's motion when masked by parallel noise (compared to orthogonal noise) above a certain "critical speed", corresponding to a spatiotemporal integration period of roughly one "dot width" per 100 ms. A noise mask whose dominant orientation is parallel with the direction of motion should be more effective than an orthogonal mask if the translating dot leaves a trailing motion streak, as the mask would produce a large and target-irrelevant response in orientation-selective neurons aligned with the motion streak and make it harder to detect the streak's presence. Several other psychophysical studies have since supported this model (Apthorp & Alais, 2009; Apthorp, Wenderoth, & Alais, 2009; Burr & Ross, 2002; Edwards & Crane, 2007; Krekelberg, Dannenberg, Hoffmann, Bremmer, & Ross, 2003; Ross, Badcock, & Hayes, 2000; Tong, Aydin, & Bedell, 2007). In addition, neurophysiological evidence suggests that there are direction-selective cells in V1 that respond preferentially to orientations parallel to their preferred direction when the motion stimulus is fast (Geisler, Albrecht, Crane, & Stern, 2001).

In the experiments reported below, we use a masking paradigm to examine how detection thresholds for 1-D luminance gratings are affected when spatiotemporally overlaid with a "streaky" motion stimulus. We use fast translating fields of Gaussian blobs as the "streaky" masks and sine-wave gratings as the target stimuli. In order to

doi: 10.1167/10.10.11 Received April 20, 2010; published August 13, 2010 ISSN 1534-7362

explore the orientation tuning properties of the mechanism encoding the motion streaks, we will systematically vary the angular difference between the target grating's orientation and the direction of motion (and consequently streak orientation) to define the orientation tuning function. We expect to obtain clear evidence of orientation tuning for streak masking because streaks are presumably encoded early in visual processing where neurons are known to be selective for orientation (Blake & Holopigian, 1985; De Valois et al., 1982; Foster, Gaska, Nagler, & Pollen, 1985; Gur, Kagan, & Snodderly, 2005; Hubel & Wiesel, 1962). We should therefore be able to reveal the tuning function of the underlying spatial channels supporting the psychophysical effects caused by motion streaks.

In Geisler's (1999) original masking experiment, the dots and mask both had very low luminance, and luminance rather than contrast thresholds were measured (even when masking was maximal, thresholds were only 9 cd/m^2). Since streaks are assumed to be due to visual integration over time, and since temporal integration occurs over a longer period at low luminances (Kelly, 1961; Roufs, 1972) and contrasts (Georgeson, 1987; Stromeyer & Martini, 2003), it is possible that the spatiotemporal dynamics of motion streaks may be different at the higher photopic luminances associated with diurnal vision, which may involve luminances up to several hundreds of cd/m^2, and the dynamics may also vary with different contrast levels. We will therefore measure orientation tuning functions for a range of mask contrasts from threshold to full contrast. In the case where gratings and streak masks are iso-oriented, this range of contrasts will also allow us to obtain threshold versus contrast (TVC or "dipper") functions that will plot grating detection thresholds as a function of the contrast of the streak pedestal.

Finally, we have previously shown tuned suppression of oriented stimuli during binocular rivalry between fast-moving fields of Gaussian blobs with orthogonal directions (Apthorp et al., 2009), which we attributed to within-channel orientation masking due to motion streaks. Because of this finding, and the fact that dichoptic masking and binocular rivalry are thought to share common cortical processes (van Boxtel, van Ee, & Erkelens, 2007), we also chose to test the orientation tuning of streak masking dichoptically and monoptically to investigate ocular specificity of any masking effects.

Methods

Participants

Participants were three experienced psychophysical observers, all of whom had normal or corrected-to-normal vision. Two were authors and the third was naive to the purpose of the experiment. All had normal stereoscopic vision as measured by the RanDot Stereo test.

Apparatus and stimuli

Stimuli were programmed in Matlab version 7.4 using the Psychophysics Toolbox (Brainard, 1997; Pelli, 1997). Participants viewed the stimuli on a Mitsubishi DiamondView 22-inch CRT monitor with a screen resolution set to 1024 × 768 pixels and a vertical refresh rate of 100 Hz, controlled by a Mac Pro computer with a dual-core Intel Xeon processor. A Cambridge Research Systems Bits++ digital-to-analogue converter was used to provide 14-bit resolution in order to enable precise measurement of low contrast thresholds. The monitor was gamma-corrected in software to achieve linearity of output. Observers viewed all stimuli though a mirror stereoscope with a total optical path of 57 cm. The mask stimuli were two drifting random dot displays, each composed of 80 Gaussian blobs with a standard deviation (*SD*) of 0.08 degrees, giving a dot diameter (defined as 4 × dot *SD*) of 0.32 degrees. Half of the dots were dark and half were light, drifting with 100% coherence on a mid-gray background. Maximum and minimum dot luminances were 67.3 and 0.26 cd/m^2 and background luminance was 33.8 cd/m^2. The dots drifted at 13.02°/s (well above Geisler's critical streak speed of one dot width per 100 ms), controlled by manipulating the

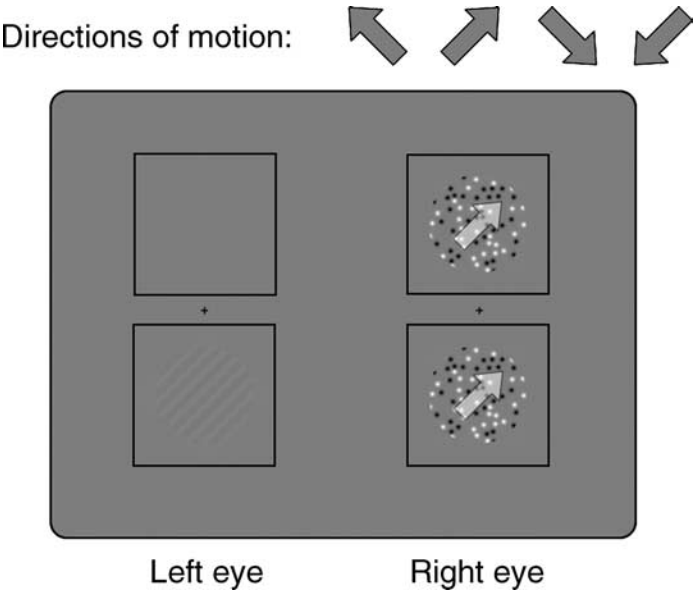

Figure 1. A schematic diagram of the procedure for Experiment 1. Probe orientation was defined relative to the direction of motion, where 0° was parallel with the motion trajectory. Four motion directions were randomly interleaved, with a range of grating orientations tested so that a tuning function could be derived. The upper and lower windows always contained the same motion direction on a given trial, and orientation was blocked. A dichoptic condition (as shown) and a monoptic condition were run in separate blocks.

pixel step size each video frame. Stimuli were presented within dark fusion squares in the upper and lower fields of the left- and right-eye views (see Figure 1), located 3.81° above and below a white fixation cross that appeared between the upper and lower fusion squares. Within the fusion squares (which were always present), stimuli appeared within virtual circular apertures 4.88° in diameter located 7.61° to the left and right of the center of the screen, which could be aligned by adjusting the stereoscope so that the left- and right-eye views were at corresponding retinal locations to allow dichoptic or monoptic presentation of mask and target. The initial position of each dot was randomly determined and all dots wrapped around the aperture.

During the test phase, the fixation cross changed to black and the test stimulus (a low-contrast sine-wave grating) appeared in either the upper or lower test aperture. Because motion streaks produced by translating Gaussian blobs do not have a unique spatial frequency (unlike a sine-wave grating), we had to determine an appropriate spatial frequency for the test grating. We did this using Geisler's "dot width" criterion whereby a Gaussian blob is assigned a width equal to four times its standard deviation. As we used a mixture of dark and light blobs on a gray background (thus leaving dark and light streaks), we chose a grating wavelength corresponding to twice the nominal blob width on the basis that a dark streak beside a light streak would correspond to that spatial period. On this basis, the spatial frequency of the test grating was set to 1.54 cyc/deg (see Figure 1, which shows a scaled version of the on-screen stimuli). The orientation tuning of the effect was investigated by rotating the grating's orientation from the motion trajectory by 10, 20, 30, 40, 60, or 90 degrees. The entire tuning function was determined at mask threshold, and at mask threshold multiples of 2, 16, 64 and full contrast. In addition to these tuning function conditions, the contrast response functions for gratings parallel to the streaks (i.e., 0° orientation) were measured more finely at mask threshold multiples of 0.5, 1, 2, 4, 8, 12, 16, 32, 64 and full mask contrast, and were measured in both the dominant and non-dominant eyes in separate blocks of trials. In all cases, mask detection thresholds were determined individually for each subject.

Procedure

Participants were given time to adjust the stereoscope to ensure correct fusion of the stimuli, using the fusion squares, after which they pressed a key to initiate trials. Conditions were blocked by orientation difference from motion for dichoptic and monoptic conditions, and by contrast threshold multiple, and the drifting Gaussian dot arrays were presented to the participant's dominant eye (eye dominance was determined by a behavioral pointing test). During each session, four directions of motion (45°, 135°, 225°, and 315°) were randomly interleaved to prevent motion adaptation from affecting the results and the grating's orientation was always defined relative to the motion trajectory. The motion was always present for 1000 ms during which the probe grating ramped on and off briefly in a temporal Gaussian window with a standard deviation of 100 ms; there was a random lag of between 10 and 200 ms between motion and probe onset times. In separate blocks, the grating could appear in the same eye as the motion stimulus (monoptic presentation) or the other eye (dichoptic presentation, as illustrated in Figure 1). In a spatial two-interval, two-alternative forced-choice task, the subject was asked to indicate whether the grating had appeared in the upper or lower aperture, and contrast thresholds for grating detection were determined in four interleaved QUEST staircases (Watson & Pelli, 1983), one for each direction of motion. Measurements were also made for grating detection without the presence of masking motion to provide an unmasked baseline threshold. The dependent variable was the elevation in grating detection threshold from the unmasked baseline, expressed in decibels:

$$M = 20 \times \log_{10}\left(\frac{T_{unmasked}}{T_{masked}}\right), \quad (1)$$

where M refers to the masking level and T refers to contrast detection threshold.

Results

The results for the orientation tuning of masking by streaks are shown in Figure 2, with the monoptic and dichoptic data plotted separately. The data are group means representing threshold elevation from baseline in decibels as a function of grating orientation, with mask contrast as a parameter. The different shades of the data points and their various symbols correspond to different levels of mask contrast (multiples of mask threshold). Evidence of masking is indicated by the elevation of the data points above 0 dB (the unmasked baseline level). Any data points falling below 0 dB indicate facilitation rather than masking (i.e., gratings were easier to detect in the presence of the "mask"). The continuous lines are best-fitting Gaussian functions of the form:

$$G = A \times \exp\left[-\frac{(\theta-\theta_0)^2}{2\sigma^2}\right] + b, \quad (2)$$

where A, σ, and b were free parameters. A represents the amplitude of the orientation-tuned masking component, and θ represents its standard deviation. The term b

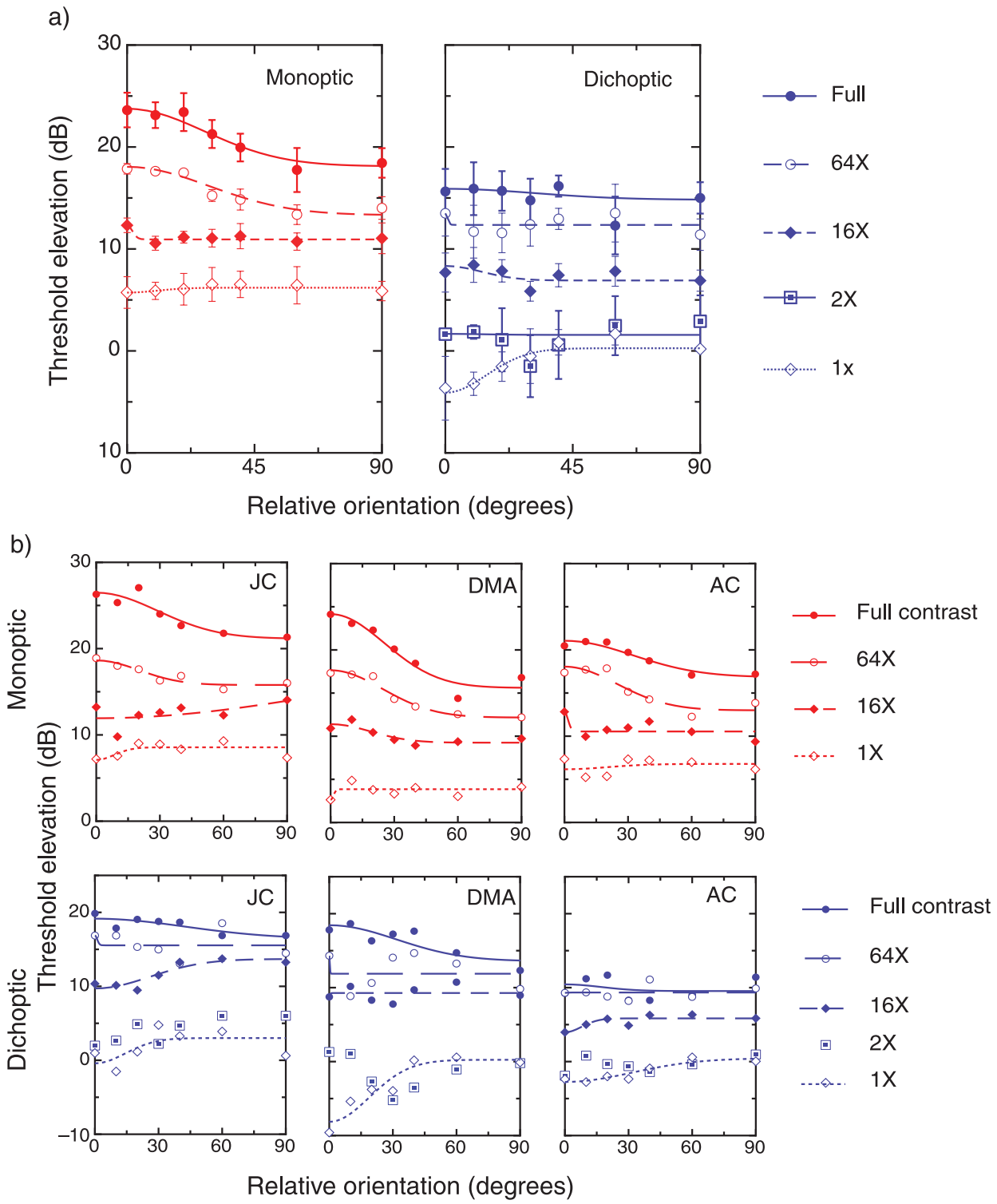

Figure 2. (a) Group means (with ±1 standard error bars) for 3 observers showing orientation tuning of streak masking for (left) monoptic and (right) dichoptic conditions. Contrast threshold elevation is plotted in decibels as a function of the orientation of the test grating relative to the motion trajectory, with contrast of the drifting dot mask as a parameter. The contrast of the drifting dot mask was standardized for observers in terms of multiples of their mask detection threshold represented by different symbols and curves. Clear evidence of orientation-tuned masking in monoptic conditions emerges as contrast increases. The only orientation-tuned component in the dichoptic conditions is a tuned facilitation when the mask is presented at threshold. (b) Individual results for the three observers for (top) monoptic and (bottom) dichoptic masking conditions. It is evident that all three observers showed very much the same pattern of results; two out of the three observers show weakly orientation-tuned masking at full contrast in the dichoptic condition, but this is not evident in the mean data.

represents an untuned (or "isotropic") threshold elevation component that has no selectivity for orientation. Note that θ in this case refers to orientation, and that θ_0 was fixed at a value of 0°, as we expected masking to be maximal when the gratings and streaks are perfectly aligned (i.e., at a relative orientation of 0°).

The expected pattern of data if masking were tuned would be a peak at 0°, where the target grating and streaks are co-oriented, and a decline in masking as the angular difference between target and mask increases. The clearest evidence of orientation-tuned masking in Figure 2 occurs in the monoptic condition, with tuned masking becoming monotonically stronger as mask contrast increases. For the two conditions with high contrast mask (full contrast and 64× threshold), the orientation tuning is clearest and the bandwidths are very similar, at 32.3° and 34°, respectively. The strength of this orientation-tuned component declines with contrast and is absent when mask contrast reaches threshold. It seems slightly odd that a baseline masking component of around 5 dB remains in this condition even at mask threshold; however, this is likely to be a result of eye dominance. We measured both dominant and non-dominant eye masking functions for two participants and found approximately 5 dB higher thresholds across all contrast levels in the non-dominant eye (see Figure 4a). It should be noted that this represents a DC shift and does not affect the bandwidth of the orientation-tuned component.

By contrast, the dichoptic condition shows no tendency for tuned masking to emerge with increased contrast, and the only orientation-tuned dichoptic component is a tuned facilitation when the mask is presented at threshold. This is an intriguing asymmetry because in the monoptic condition masks presented at threshold produced no tuned effects at all, and more generally, no facilitation is evident at any monoptic contrast. The dichoptic threshold facilitation is more tightly tuned for orientation than the monoptic masking tunings, having approximately half the orientation bandwidth of the monoptic effects, with a bandwidth of 17.1°.

Figure 3 plots the baseline elevation (upper panel) and amplitude (lower panel) parameters from the best-fitting Gaussians shown in Figure 2. In the top panel, the greater overall strength of monoptic masking relative to dichoptic masking is evidenced by the higher level of the untuned baseline component at each level of contrast. A two-way, within-subjects repeated-measures ANOVA on the baseline component, however, showed no significant main effect of ocular mode of presentation but a significant effect of contrast ($F(3, 6) = 108.66$, $p < 0.001$). There was a significant interaction between contrast and ocular condition ($F(3, 6) = 7.13$, $p = 0.011$). There were significant linear ($F(1, 2) = 149.83$, $p = 0.007$) and cubic ($F(1, 2) = 32$, $p = 0.03$) trends for contrast, and a near-significant cubic trend ($F(1, 2) = 14.86$, $p = 0.061$) for the interaction. Thus, the difference between the baseline component in monoptic and dichoptic conditions varies as a function of contrast, with greater differences at threshold and full contrast than in the intermediate conditions.

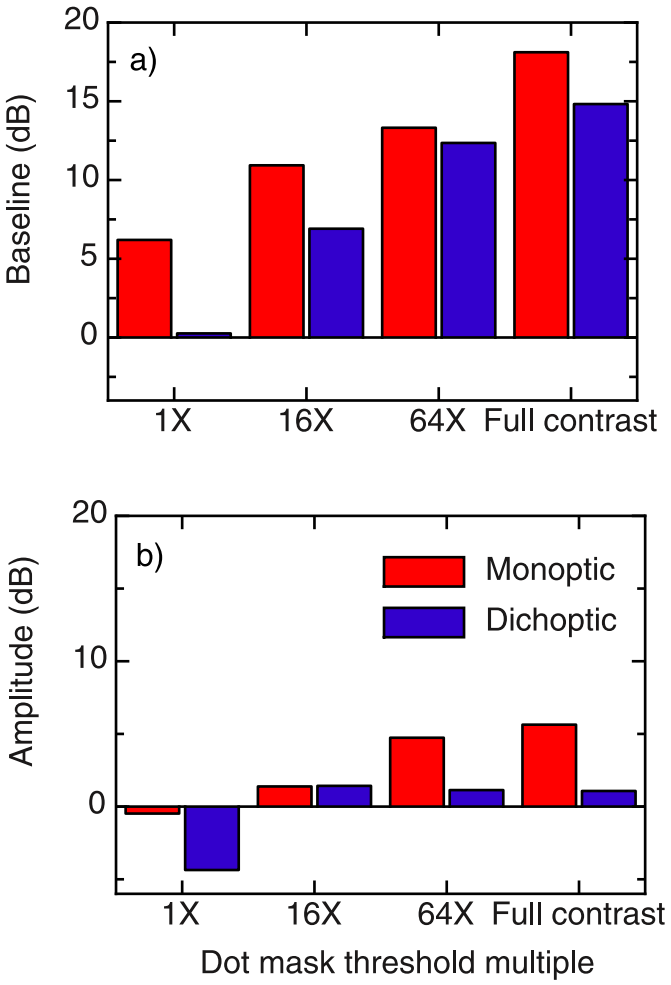

Figure 3. Parameters for the Gaussian best fits to the data shown in Figure 2. The upper panel shows the Gaussian baseline (corresponding to the unoriented masking component) and amplitude (the orientation-tuned masking component).

The bottom panel plots the amplitude of the orientation-tuned components and shows a different pattern for dichoptic and monoptic data in the relationship between orientation-tuned amplitude and mask contrast. The monoptic masking functions show a clear monotonic increase (from 0 dB to 6 dB) in the amplitude of the orientation-tuned component with increasing contrast of the translating dot mask, whereas the dichoptic functions show tuned facilitation at threshold, but less of an increase with higher contrasts. A two-way repeated-measures ANOVA as above showed a main effect of eye condition ($F(1, 2) = 70.28$, $p = 0.014$) and of contrast ($F(3, 6) = 12.52$, $p = 0.0005$). There was no significant interaction between eye condition and contrast for the amplitude component.

To further explore the masking and facilitation effects, we measured the entire contrast response function for parallel gratings (i.e., 0° orientation relative to streaks) as a function of mask contrast, for both monoptic and

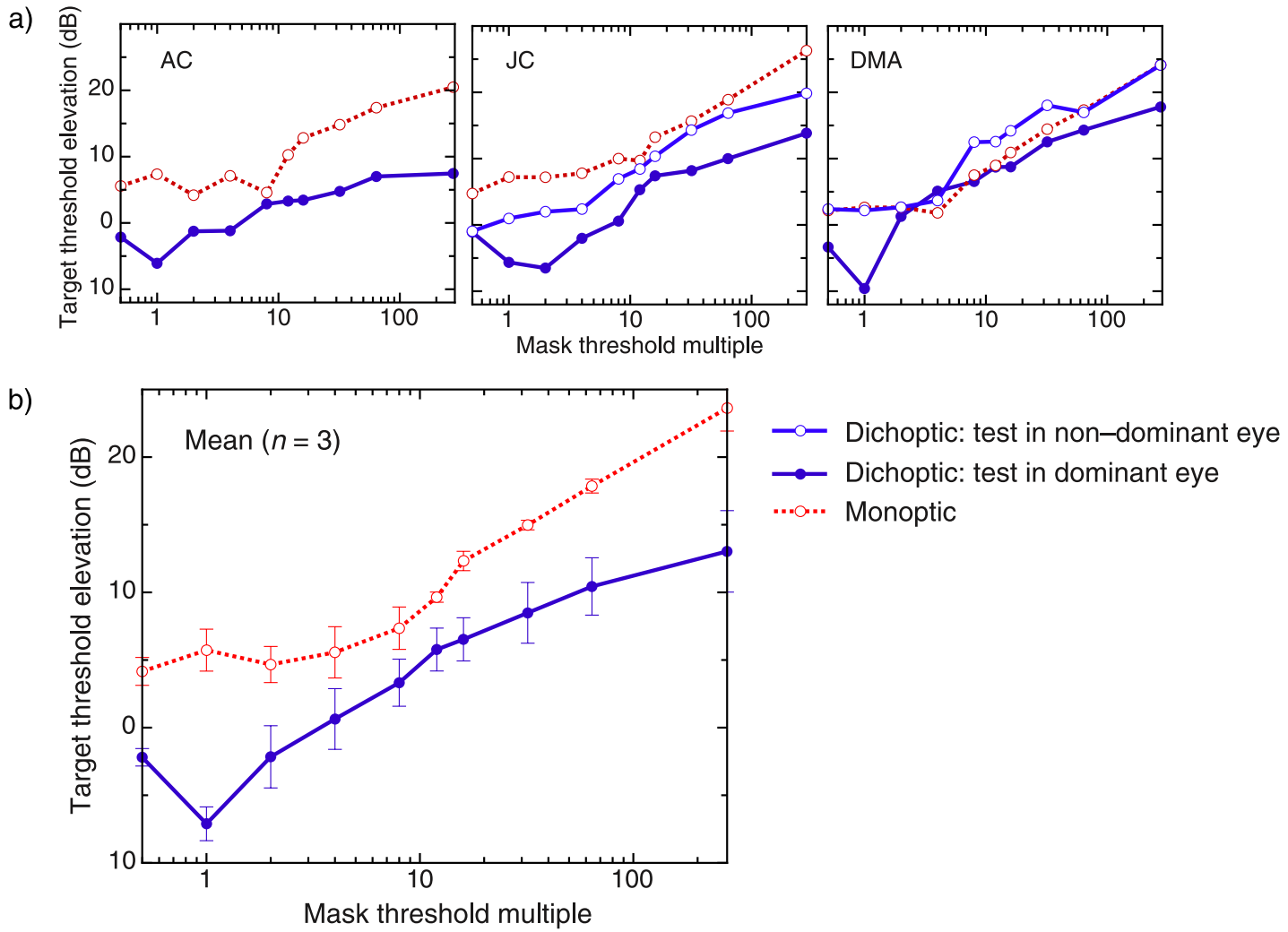

Figure 4. (a) Individual contrast response functions for the 3 subjects. Blue lines show dichoptic CRFs. For two participants, we measured the function with the test grating in the dominant and non-dominant eye, and facilitation was seen only in the former case. Note also that threshold elevation is somewhat higher overall when the test is in the non-dominant eye. (b) Contrast response functions for monoptic and dichoptic conditions, averaged across three subjects, for masking by parallel dot motion as a function of mask (dot) contrast.

dichoptic conditions. Figure 4 plots the mean dichoptic and monoptic masking functions for the three observers. The facilitation effect seen in the dichoptic condition in Figure 2 is evident again, with grating detection threshold actually improving (i.e., facilitation) when masks are presented to the other eye at detection threshold. This pattern of dichoptic facilitation for threshold masks was seen consistently in all three observers. When tested at an even lower mask contrast level, grating thresholds returned to the level of the unmasked baseline, thereby exhibiting the shape of the classical "dipper function". When the contrast response function for parallel gratings was measured in the monoptic condition, there was no facilitation, consistent with the absence of any facilitation in the monoptic data in Figure 2.

The masking results plotted in Figures 2 and 3 indicate a clear orientation-tuned component. Although the masks of translating dots we used do not physically contain orientation, the sluggish temporal response of the visual system predictably leads to the stimuli becoming smeared over time so that the individual dots will leave elongated trails known as "motion streaks" (Geisler, 1999). It is thought that the temporal integration period giving rise to this smearing is about 100 ms in early visual cortex (Burr, 1981; Snowden & Braddick, 1991) and it is important therefore to know exactly what orientation information is contained in the translating dot masks when they have been averaged over this period. To determine this, we summed 10 consecutive animation frames (i.e., a motion sequence of 100 ms) and conducted a Fourier analysis on the resulting image. For comparison, we show the results of the same analyses on a single frame of dots.

The summed image was transformed into frequency space using a fast Fourier transform. The amplitude

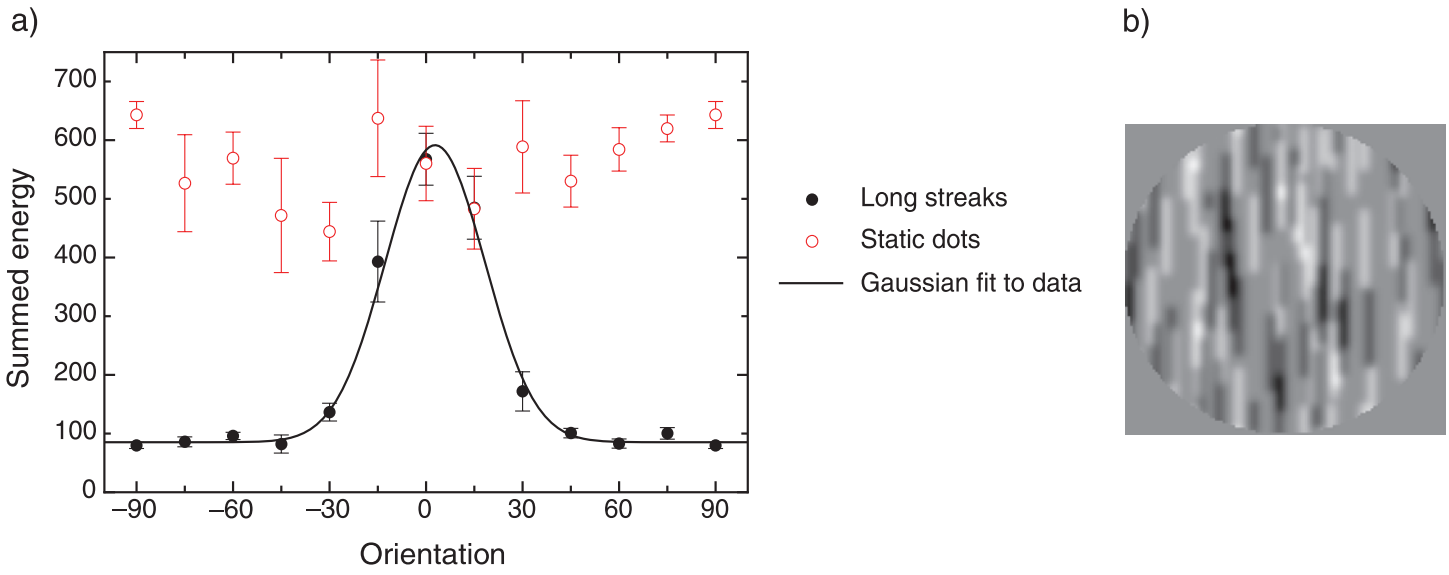

Figure 5. (a) The amplitude spectrum of a summed 100-ms motion sequence (see text for details) as a function of orientation relative to the direction of motion. The summed images were produced by summing 10 frames of the motion sequence to imitate motion streaks produced by a temporal integration period of 100 ms. Only the energy in a one-octave spatial bandwidth centered on 1.54 cyc/deg (the spatial frequency of the test grating) is shown, and orientation is binned into 15° intervals. For comparison, the same analysis of orientation is shown for a single frame of dots. The distribution of the energy across orientation for the summed motion sequence is well fitted by a Gaussian function with a half-bandwidth at half-height of 18.2° (*SD* = 0.8°), and a peak at 2.8° (*SD* 1.2°), close to the axis of motion (0°). The energy contained in the single dot frame was approximately equal at all orientations. (b) An example of the summed stimuli used for the analysis.

spectrum was then spatially filtered using an isotropic log-Gaussian filter to pass a band of spatial energy one octave wide and centered on the spatial frequency of the test grating (i.e., 1.54 cyc/deg). The distribution of energy as a function of orientation was then recorded for this spatial passband. Because the entire motion stimulus was 1000 ms in duration, we repeated the 100-ms sampling process many times, randomly choosing a new starting point for the sequence on every iteration. An average of 400 iterations of this procedure produced the results shown in Figure 5. The left panel shows the distribution of energy as a function of orientation, with orientation binned into 15° intervals. The summed 100-ms motion sequence contains a very strong orientation bias along the axis of motion (indicated by 0°) and has very little energy at other orientations. By comparison, oriented energy in the static image is approximately uniformly distributed. The continuous line shows the best-fitting Gaussian function for the summed motion stimulus.

It is interesting to compare the orientation tuning of the amplitude spectrum of the summed motion image with the orientation tunings obtained psychophysically, as shown in Figure 6. Figure 6a replots two of the orientation-tuned functions from Figure 2, the full-contrast monoptic data and the low-contrast dichoptic data, and the Fourier amplitude spectrum of the summed "streak" images from Figure 5. To facilitate comparison, the psychophysical data have been normalized by aligning the maximum of the monoptic and dichoptic data with the maximum of the normalized amplitude spectrum (this does not alter the bandwidths). The orientation-tuned component of the monoptic masking function is markedly broader (bandwidth = 33°) than the Fourier analysis reveals in the summed motion image (bandwidth = 18.2°), suggesting that the neural processes underlying monoptic masking, presumably orientation channels in primary visual cortex (Barlow, 1958; Campbell & Kulikowski, 1966; Snowden, 1991; Watson, 1979), have an orientation resolution that is broader than the orientations contained in the physical stimulus. In contrast, the dichoptic facilitation function (bandwidth = 17°) has an orientation tuning that is very similar to that of the stimulus, suggesting that the stimulus provides the limit to the tuning function in the dichoptic case.

An alternative explanation for the differing bandwidths is illustrated in Figure 6b. It is possible that, as suggested in the Introduction section, temporal integration times for streaks under full-contrast masking conditions might be different from those at threshold contrasts (Georgeson, 1987; Stromeyer & Martini, 2003). Accordingly, we created summed stimuli for different periods of temporal integration, from 30 to 100 ms, performed fast Fourier transforms on these stimuli, and analyzed the distribution of energy in the amplitude spectra of these summed stimuli of different lengths. It is evident from Figure 6b that the bandwidth of the full-contrast monoptic masking function most closely matches that of a stimulus integrated over around 40 ms. This is markedly different from

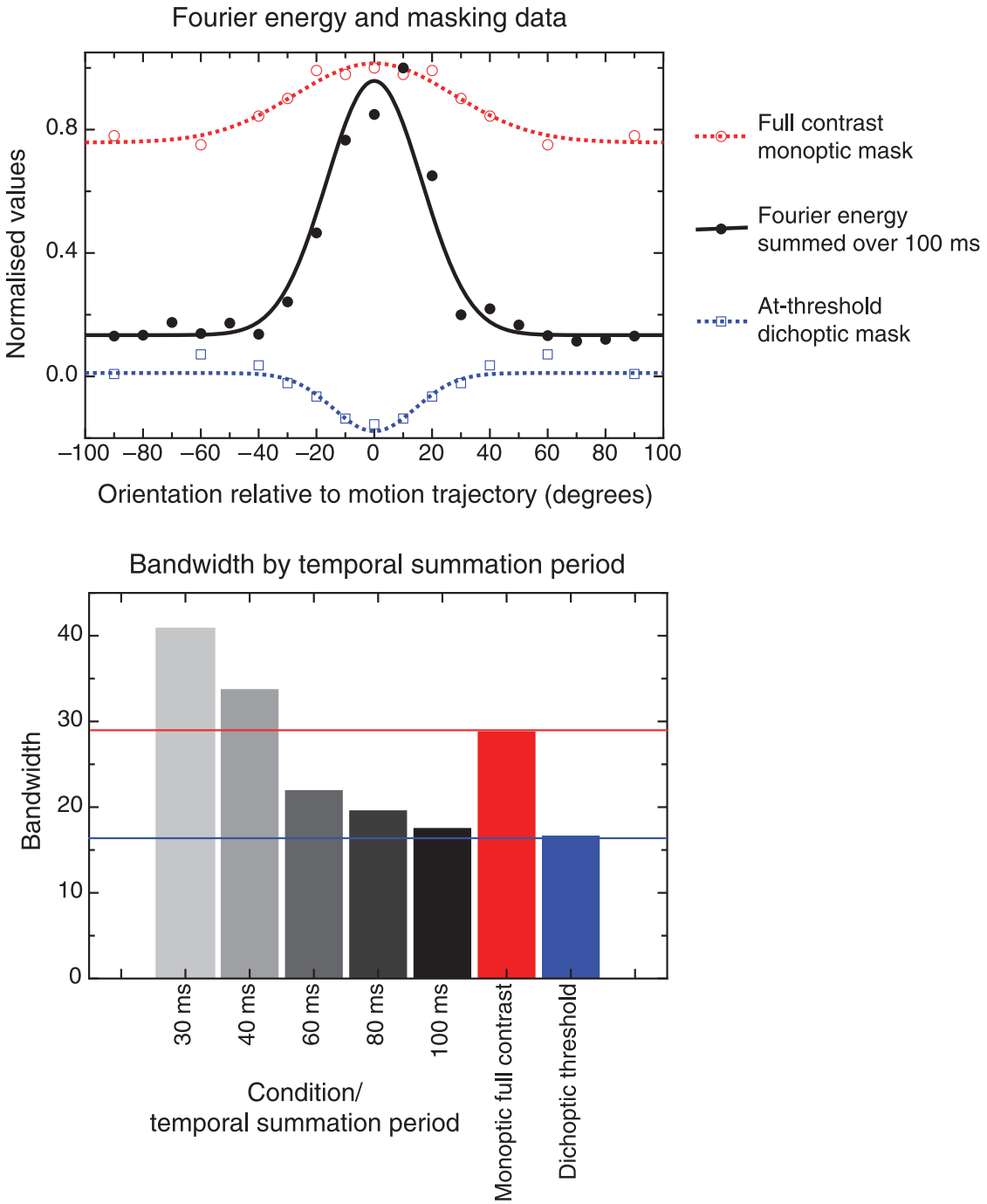

Figure 6. (a) A comparison of the oriented energy in the stimulus, summed over 100 ms (where 0° indicates the axis of motion), and the orientation tuning of the psychophysically derived masking functions. The masking data have been normalized to the maximum of the Fourier plot to facilitate comparison. The monoptic data are more broadly tuned for orientation than the physical stimulus if assuming a 100-ms integration period. (b) A comparison of the bandwidths of the full-contrast and at-threshold masking functions with the bandwidths of Fourier analyses of the motion stimulus summed over different temporal intervals. The full-contrast masking bandwidth corresponds most closely with the 40-ms integration period, while dichoptic threshold facilitation mirrors the bandwidth of a stimulus summed over 100 ms.

the bandwidth of the threshold facilitation function, which, as mentioned above, is very close to that of a stimulus integrated over 100 ms.

Discussion

The results of this experiment demonstrate that strong and orientation-dependent masking of grating detection occurs when overlaid with a fast, translating field of Gaussian blobs. Our findings are therefore generally consistent with Geisler's original observation that a dynamic one-dimensional noise stimulus masks motion when the noise is parallel (rather than orthogonal) to the motion direction (Geisler, 1999). There are several important aspects in our data that have not been previously shown. First, Geisler's masking experiment used oriented dynamic noise to mask motion, whereas we have shown the inverse—that fast "streaky" motion effectively masks orientation. There is a somewhat similar result in the literature: Westheimer and Wehrhahn (1994) showed flanking fast-moving dots impaired orientation discrimination of a single line. This study was carried out before the recent resurgence of interest in motion streaks, but the results may be due to very much the same mechanisms. Second, we have systematically explored the orientation dependence of masking by motion streaks and have done so as a function of mask contrast, both dichoptically and monoptically (see Figure 2). In our discussion, we will first focus on the strong unoriented masking component evident in the baseline elevations of Figure 2, before discussing the contrasting patterns of orientation-tuned masking between the dichoptic and monoptic conditions.

A consistent result in the dichoptic and monoptic conditions was the increase in the level of the unoriented masking component. This increase was linear with the log of mask contrast, for both monoptic and dichoptic conditions. Best-fitting straight lines had slopes of 4.14 (monoptic, $r^2 = 0.82$) and 5.07 (dichoptic, $r^2 = 0.77$). These observations accord with those of previous studies that have used traditional sinusoidal grating stimuli as targets and masks and have also found cross-orientation effects that increase with contrast, both monoptically and dichoptically (Meese & Baker, 2009; Meese & Holmes, 2007) In our study, the total masking effect (that is, the orientation-tuned plus untuned components) is largely due to this untuned cross-orientation component. Looking at the monoptic data in Figure 2, the two low-contrast masking functions exhibit no discernable orientation tuning and so are entirely attributable to the untuned masking effect, and even though the two high-contrast conditions do show orientation tuning, a majority of the total masking is untuned for orientation. This is clearly evident in Figure 3 where the tuned component is smaller than the untuned component by three to one. In the dichoptic data, with the exception of the tuned facilitation at threshold (discussed below), masking is generally attributable to the untuned component.

What is the likely source of this robust orientation-untuned (or "isotropic") masking effect? Evidence from both psychophysical and neurophysiological studies indicates that cross-orientation masking is very strong when the temporal frequency of the oriented masking stimulus exceeds that of an orthogonally oriented target (Allison, Smith, & Bonds, 2001; Boynton & Foley, 1999; Cass & Alais, 2006; Cass, Alais, Spehar, & Bex, 2009; Meier & Carandini, 2002). By comparison, when the temporal rate of target modulation exceeds that of the masking stimulus, cross-orientation masking is relatively weak. In our experiments, there is a fundamental asymmetry between the temporal frequency content of the targets and masks in that the targets are stationary while the masks are moving. While it is true that the target appears and disappears during the course of each trial, and thus must contain a range of temporal frequencies, these were attenuated by presenting the target in a Gaussian temporal envelope. We performed a Fourier analysis to assess the temporal frequencies present in the probe grating and found that the range of frequencies was very low, centered around 0, and with a standard deviation of 1.9 Hz. Given the temporal frequency of the mask exceeds that of the target, strong cross-orientation masking would be expected. Consistent with these earlier studies that have shown transiently biased cross-orientation masking, the isotropic masking in our study probably also results from magnocellular (motion-driven) processes. The specific neurophysiological basis of cross-orientation masking has been a matter of considerable debate for more than a quarter of a century (Freeman, Durand, Kiper, & Carandini, 2002; Macevoy, Tucker, & Fitzpatrick, 2009; Tucker & Fitzpatrick, 2006), with the neural locus of cross-orientation masking being variously attributed to pre-cortical (Carandini et al., 1997; Freeman et al., 2002; Priebe & Ferster, 2002) and/or intra-cortical (Allison et al., 2001; Heeger, 1992; Morrone, Burr, & Speed, 1987) mechanisms.

The other masking component central to the aims of this study is the orientation-tuned component. In the monoptic data, a clear orientation-tuned component becomes apparent as mask contrast increases (see Figures 2a and 3b). Orientation-dependent elevations in detection threshold have been consistently reported in masking studies since the late 1960s (Blake & Holopigian, 1985; Bonds, 1989; Campbell & Kulikowski, 1966; Phillips & Wilson, 1984; Ross & Speed, 1991). Estimates of orientation tuning based on Gaussian bandwidths (half-widths at half-height) typically vary in the range of 7–40°, although depending on approach and methodology estimates of orientation bandwidth can vary far more widely (for a meta-analysis, see Cass, Stuit, Bex, & Alais, 2009). Recent evidence, however, indicates that orientation masking functions can be decomposed into orientation-tuned and -untuned components, and that by this analysis the bandwidths of the

tuned components are approximately constant over a wide range of spatial and temporal frequencies at ~30° (Cass, Stuit et al., 2009; Meese & Holmes, 2003). The orientation-tuned components in our monoptic condition have a bandwidth of ~33° and therefore fit well with these latter studies. In the dichoptic condition, the orientation-tuned masking components were only observed for two out of the three subjects. At threshold levels of mask contrast, however, tuned *facilitation* was evident for all three subjects. The orientation bandwidth of this tuned dichoptic facilitation was far narrower than that of the tuned monoptic masking at approximately 17° compared to the 33° bandwidth of the monoptic components. Interestingly, the bandwidth of this orientation-tuned facilitative component accords closely with the orientation content of the streak mask (see Figure 6a) and therefore suggests that the facilitative tuning may be determined by the stimulus (i.e., an external factor) rather than necessarily indicating a lower bound estimate of dichoptic summative bandwidths (Baker & Meese, 2007).

An alternative explanation for the differing bandwidths of monoptic masking and dichoptic facilitation is illustrated in Figure 6b. It is possible that the effective stimulus for masking is actually integrated over a much shorter period than that for facilitation, so that "mask" streaks are perhaps only integrated over around 40 ms, in which case the bandwidth of the stimulus would match the bandwidth of the masking function. However, this does not accord with Geisler's findings that the "critical dot speed", where masking by parallel and orthogonal noise began to differ, was equivalent to approximately one dot width per 100 ms for a range of different dot sizes. The difference may be due to shorter integration times at higher mean luminance (Kelly, 1961; Roufs, 1972), but the mean luminance was the same throughout our experiment. Alternatively, dichoptic and monoptic masking have very different temporal profiles. It would be interesting to investigate this question more directly, perhaps by probing orientation sensitivity at different time points during a motion sequence.

It has previously been suggested that dichoptic masking and binocular rivalry may share common cortical mechanisms (van Boxtel et al., 2007). Since we have previously measured the orientation tuning of grating suppression during motion rivalry (Apthorp et al., 2009), it would be interesting to compare the bandwidths from that experiment with those from this study. Curiously, orientation-tuned rivalry suppression was considerably narrower in bandwidth (~22°) than both our monoptic and dichoptic masking tuning (~33°), and in addition, there seems to have been a greater orientation-tuned component in rivalry.

The differences between the monoptic and dichoptic data led us to measure full-contrast response functions for gratings and streaks aligned in parallel both monoptically and dichoptically (Figure 4). Interestingly, the obtained masking functions appear at odds with those seen in previous studies using gratings for target and mask (Baker & Meese, 2007; Meese, Georgeson, & Baker, 2006). Typically, these masking studies show: (i) more facilitation (i.e., a more prevalent "dip" at low mask contrast) in monoptic conditions, and (ii) greater threshold elevation (i.e., steeper dipper handles) at intermediate to high masking contrasts in dichoptic conditions (Meese et al., 2006). By contrast, our data show the opposite pattern: facilitation was only evident dichoptically (not monoptically), and threshold elevation for our streak masks was greater monoptically than dichoptically at all mask contrasts. A key difference between the streak stimuli used in our study and previous studies employing gratings concerns the phase relationship between target and mask. Both Maehara and Goryo (2005) and Meese et al. (2006) used target and masking stimuli with matching spatial phase (as well as orientation, spatial frequency, and spatiotemporal location). The phase relationship between our target and mask stimuli, however, varied randomly across trials, as well as across the stimuli on any given trial (because the streak image is spatially broadband, unlike a grating). If these typical masking effects are in fact contingent upon targets and masks being in-phase, then this could underlie the different pattern of results we obtained using a broadband "streak" mask. More specifically, the facilitative region of the contrast masking function is often attributed to within-channel summation at low contrast that is both phase- and orientation-selective (Meese et al., 2006). Given the random phase structure of our masking stimuli, we could not expect our target grating and streak mask to reliably summate to produce an increased response in a phase-sensitive detection mechanism.

If the broadband nature of the mask prevents monoptic facilitation, what causes the facilitation when the same stimuli are presented dichoptically? Baker and Meese (2007) reported that dichoptic summation effects occurred when target and masking stimuli were presented in the same spatial phase but did not occur when presented in anti-phase. The random phase structure of our mask means the target and masking stimuli are unlikely to have been completely in-phase or in anti-phase. In fact, a probable consequence of this random phase structure is the presence of random variation in binocular disparity across the dichoptically combined target and masking image. We propose that the narrowband dichoptic facilitation we observed may arise from summation within binocular disparity-selective channels (Cormack, Stevenson, & Schor, 1993; Hess, Kingdom, & Ziegler, 1999; Hibbard, 2005). Based on this interpretation of our dichoptic facilitation effects, we would predict that similar dichoptic facilitation should occur using traditional grating stimuli for a large range of relative phases, provided the gratings were not perfectly in-phase or in anti-phase. Finally, why are the dichoptic masking functions in Figure 4 not as steep as those obtained with gratings (Baker & Meese, 2007; Meese et al., 2006)? We speculate that this may be due to the strong isotropic masking response

effectively weakening the visual response to the oriented streak information in the mask (see Figure 6), rendering the oriented signal too weak to elicit strong threshold elevation.

A final question on which our data can shed some light concerns the contrast level at which streaks begin to function as oriented stimuli. Streaks are inherently a low-contrast stimulus because they are formed by a single dot that translates spatially during the course of the temporal integration period. Unlike a stationary dot, which activates a single point within a receptive field for the entire temporal integration period, a translating dot activates a series of points across the receptive field, each for only a fraction of the integration period. This reduces the intensity of all points along the streak's length (in a speed-dependent manner) and means that a streak will always have a lower "effective contrast" than the image that forms it. Looking at the monoptic data in Figure 3, it is clear that contrast at maximum and at 64× threshold is sufficient to produce oriented masking, whereas contrast at 16× threshold is not. Corroborating this, the more finely sampled contrast response function in Figure 4 has a flat floor at low contrasts and begins to accelerate at around 10–15 times threshold. This suggests that, at least in the context of masking and at the speed we used (13°/s), the streaks require about 15× threshold to become effective.

What are the implications of the data for motion streak models? First, the high level of untuned temporal-frequency masking is interesting: could this imply that, under normal circumstances, the oriented trace left by fast motion might be masked by surrounding fast-moving objects, and so may not be as useful as previously thought? Alternatively, it could be argued that masked stimuli can still be effective in the absence of awareness (Clifford & Harris, 2005). Future research examining the dependency of spatio-temporal factors on orientation-tuned and untuned masking components is likely to shed light on this; thus a fast-moving object would usually be surrounded by slow or static scene elements, and its "streak" would be less likely to be masked. Second, the surprising differences between dichoptic and monoptic masking suggest that there may be dynamics in the binocular combination of motion streak information with temporal frequency or speed information that remain to be explored. Third, the tuning comparisons between our data and the temporally summed stimuli suggest that the temporal integration time for motion streaks under normal lighting conditions may be a great deal shorter than previously assumed, although this remains to be directly tested.

Overall, the patterns of data presented above add to the emerging body of evidence for motion streaks and also uncover some interesting new aspects. The masking of simple, one-dimensional grating stimuli by translating dots has not previously been shown. The results illustrate that the oriented trace left by fast translating dots is likely to be mediated by the same orientation- and phase-selective channels as inferred from previous masking studies employing traditional grating stimuli. Importantly, we show that although the streak pattern left behind by the translating dots is most likely to be narrowly orientation tuned (see Figure 6a), the effects of the streaks as a mask show the reverse pattern, with far greater masking associated with an orientation-untuned component that is presumably similar to transient cross-orientation masking identified in previous studies that have used gratings as both target and mask.

Acknowledgments

We would like to thank David Burr and an anonymous reviewer for their helpful comments on the manuscript.

Author John Cass was supported by a Discovery Project (DP0774697) awarded by the Australian Research Council.

Author David Alais was supported by a Discovery Project (DP0878371) awarded by the Australian Research Council.

Commercial relationships: none.
Corresponding author: Deborah Apthorp.
Email: deborah.apthorp@sydney.edu.au.
Address: School of Psychology, University of Sydney, Sydney, NSW, Australia.

References

Adelson, E. H., & Bergen, J. R. (1985). Spatiotemporal energy models for the perception of motion. *Journal of the Optical Society of America A, Optics and Image Science, 2,* 284–299.

Allison, J. D., Smith, K. R., & Bonds, A. B. (2001). Temporal-frequency tuning of cross-orientation suppression in the cat striate cortex. *Visual Neuroscience, 18,* 941–948.

Apthorp, D., & Alais, D. (2009). Tilt aftereffects and tilt illusions induced by fast translational motion: Evidence for motion streaks. *Journal of Vision, 9*(1):27, 1–11, http://www.journalofvision.org/content/9/1/27, doi:10.1167/9.1.27. [PubMed] [Article]

Apthorp, D., Wenderoth, P., & Alais, D. (2009). Motion streaks in fast motion rivalry cause orientation-selective suppression. *Journal of Vision, 9*(5):10, 1–14, http://www.journalofvision.org/content/9/5/10, doi:10.1167/9.5.10. [PubMed] [Article]

Baker, D., & Meese, T. (2007). Binocular contrast interactions: Dichoptic masking is not a single process. *Vision Research, 47,* 3096–3107.

Barlow, H. B. (1958). Temporal and spatial summation in human vision at different background intensities. *The Journal of Physiology, 141,* 337–350.

Blake, R., & Holopigian, K. (1985). Orientation selectivity in cats and humans assessed by masking. *Vision Research, 25,* 1459–1467.

Bonds, A. (1989). Role of inhibition in the specification of orientation selectivity of cells in the cat striate cortex. *Visual Neuroscience, 2,* 41–55.

Boynton, G. M., & Foley, J. M. (1999). Temporal sensitivity of human luminance pattern mechanisms determined by masking with temporally modulated stimuli. *Vision Research, 39,* 1641–1656.

Brainard, D. H. (1997). The psychophysics toolbox. *Spatial Vision, 10,* 433–436.

Burr, D. (1981). Temporal summation of moving images by the human visual system. *Proceedings of the Royal Society of London B: Biological Sciences, 211,* 321–339.

Burr, D., & Ross, J. (2002). Direct evidence that "speedlines" influence motion mechanisms. *Journal of Neuroscience, 22,* 8661–8664.

Campbell, F. W., & Kulikowski, J. J. (1966). Orientational selectivity of the human visual system. *The Journal of Physiology, 187,* 437–445.

Carandini, M., Heeger, D. J., & Movshon, J. A. (1997). Linearity and normalization in simple cells of the macaque primary visual cortex. *Journal of Neuroscience, 17,* 8621–8644.

Cass, J., & Alais, D. (2006). Evidence for two interacting temporal channels in human visual processing. *Vision Research, 46,* 2859–2868.

Cass, J., Alais, D., Spehar, B., & Bex, P. J. (2009). Temporal whitening: Transient noise perceptually equalizes the 1/f temporal amplitude spectrum. *Journal of Vision, 9*(10):12, 1–19, http://www.journalofvision.org/content/9/10/12, doi:10.1167/9.10.12. [PubMed] [Article]

Cass, J., Stuit, S., Bex, P., & Alais, D. (2009). Orientation bandwidths are invariant across spatiotemporal frequency after isotropic components are removed. *Journal of Vision, 9*(12):17, 1–14, http://www.journalofvision.org/content/9/12/17, doi:10.1167/9.12.17. [PubMed] [Article]

Clifford, C., & Harris, J. (2005). Contextual modulation outside of awareness. *Current Biology, 15,* 574–578.

Cormack, L. K., Stevenson, S. B., & Schor, C. M. (1993). Disparity-tuned channels of the human visual system. *Visual Neuroscience, 10,* 585–596.

De Valois, R., Yund, E., & Hepler, N. (1982). The orientation and direction selectivity of cells in macaque visual cortex. *Vision Research, 22,* 531–544.

Edwards, M., & Crane, M. (2007). Motion streaks improve motion detection. *Vision Research, 47,* 828–833.

Foster, K., Gaska, J., Nagler, M., & Pollen, D. (1985). Spatial and temporal frequency selectivity of neurones in visual cortical areas V1 and V2 of the macaque monkey. *The Journal of Physiology, 365,* 331–363.

Freeman, T. C. B., Durand, S., Kiper, D. C., & Carandini, M. (2002). Suppression without inhibition in visual cortex. *Neuron, 35,* 759–771.

Geisler, W. S. (1999). Motion streaks provide a spatial code for motion direction. *Nature, 400,* 65–69.

Geisler, W. S., Albrecht, D. G., Crane, A. M., & Stern, L. (2001). Motion direction signals in the primary visual cortex of cat and monkey. *Visual Neuroscience, 18,* 501–516.

Georgeson, M. A. (1987). Temporal properties of spatial contrast vision. *Vision Research, 27,* 765–780.

Gur, M., Kagan, I., & Snodderly, D. M. (2005). Orientation and direction selectivity of neurons in V1 of alert monkeys: Functional relationships and laminar distributions. *Cerebral Cortex, 15,* 1207–1221.

Heeger, D. J. (1992). Normalization of cell responses in cat striate cortex. *Visual Neuroscience, 9,* 181–197.

Hess, R. F., Kingdom, F. A., & Ziegler, L. R. (1999). On the relationship between the spatial channels for luminance and disparity processing. *Vision Research, 39,* 559–568.

Hibbard, P. B. (2005). The orientation bandwidth of cyclopean channels. *Vision Research, 45,* 2780–2785.

Hubel, D. H., & Wiesel, T. N. (1962). Receptive fields, binocular interaction and functional architecture in cat's visual cortex. *The Journal of Physiology, 160,* 106–154.

Kelly, D. H. (1961). Visual response to time-dependent stimuli. I. Amplitude sensitivity measurements. *Journal of the Optical Society of America A, Optics, Image Science, and Vision, 51,* 422–429.

Krekelberg, B., Dannenberg, S., Hoffmann, K.-P., Bremmer, F., & Ross, J. (2003). Neural correlates of implied motion. *Nature, 424,* 674–677.

Macevoy, S. P., Tucker, T. R., & Fitzpatrick, D. (2009). A precise form of divisive suppression supports population coding in the primary visual cortex. *Nature Neuroscience, 12,* 637.

Maehara, G., & Goryo, K. (2005). Binocular, monocular and dichoptic pattern masking. *Optical Review, 12,* 76–81.

Meese, T. S., & Baker, D. H. (2009). Cross-orientation masking is speed invariant between ocular pathways but speed dependent within them. *Journal of Vision, 9*(5):2, 1–15, http://www.journalofvision.org/content/9/5/2, doi:10.1167/9.5.2. [PubMed] [Article]

Meese, T. S., Georgeson, M. A., & Baker, D. H. (2006). Binocular contrast vision at and above threshold. *Journal of Vision, 6*(11):7, 1224–1243, http://www.journalofvision.org/content/6/11/7, doi:10.1167/6.11.7. [PubMed] [Article]

Meese, T. S., & Holmes, D. J. (2003). Orientation-masking: Suppression and mechanism bandwidths. *Perception, 32,* 388.

Meese, T. S., & Holmes, D. J. (2007). Spatial and temporal dependencies of cross-orientation suppression in human vision. *Proceedings of the Royal Academy B: Biological Sciences, 274,* 127–136.

Meier, L., & Carandini, M. (2002). Masking by fast gratings. *Journal of Vision, 2*(4):2, 293–301, http://www.journalofvision.org/content/2/4/2, doi:10.1167/2.4.2. [PubMed] [Article]

Morrone, M. C., Burr, D. C., & Speed, H. D. (1987). Cross-orientation inhibition in cat is GABA mediated. *Experimental Brain Research, 67,* 635–644.

Pelli, D. G. (1997). The VideoToolbox software for visual psychophysics: Transforming numbers into movies. *Spatial Vision, 10,* 437–442.

Phillips, G. C., & Wilson, H. R. (1984). Orientation bandwidths of spatial mechanisms measured by masking. *Journal of the Optical Society of America A, Optics and Image Science, 1,* 226–232.

Priebe, N. J., & Ferster, D. (2002). A new mechanism for neuronal gain control (or how the gain in brains has mainly been explained). *Neuron, 35,* 602–604.

Ross, J., Badcock, D. R., & Hayes, A. (2000). Coherent global motion in the absence of coherent velocity signals. *Current Biology, 10,* 679–682.

Ross, J., & Speed, H. (1991). Contrast adaptation and contrast masking in human vision. *Proceedings of the Royal Society B: Biological Sciences, 246,* 61–69.

Roufs, J. A. (1972). Dynamic properties of vision. I. Experimental relationships between flicker and flash thresholds. *Vision Research, 12,* 261–278.

Snowden, R. J. (1991). Measurement of visual channels by contrast adaptation. *Proceedings of the Royal Academy B: Biological Sciences, 246,* 53–59.

Snowden, R. J., & Braddick, O. (1991). The temporal integration and resolution of velocity signals. *Vision Research, 31,* 907–914.

Stromeyer, C., & Martini, P. (2003). Human temporal impulse response speeds up with increased stimulus contrast. *Vision Research, 43,* 285–298.

Tong, J., Aydin, M., & Bedell, H. E. (2007). Direction-of-motion discrimination is facilitated by visible motion smear. *Perception & Psychophysics, 69,* 48–55.

Tucker, T. R., & Fitzpatrick, D. (2006). Luminance-evoked inhibition in primary visual cortex: A transient veto of simultaneous and ongoing response. *Journal of Neuroscience, 26,* 13537–13547.

van Boxtel, J., van Ee, R., & Erkelens, C. (2007). Dichoptic masking and binocular rivalry share common perceptual dynamics. *Journal of Vision, 7*(14):3, 1–11, http://www.journalofvision.org/content/7/14/3, doi:10.1167/7.14.3. [PubMed] [Article]

van Santen, J. P., & Sperling, G. (1985). Elaborated Reichardt detectors. *Journal of the Optical Society of America A, Optics and Image Science, 2,* 300–321.

Watson, A. B. (1979). Probability summation over time. *Vision Research, 19,* 515–522.

Watson, A. B., & Ahumada, A. J., Jr. (1985). Model of human visual-motion sensing. *Journal of the Optical Society of America A, Optics and Image Science, 2,* 322–341.

Watson, A. B., & Pelli, D. G. (1983). QUEST: A Bayesian adaptive psychometric method. *Perception & Psychophysics, 33,* 113–120.

Westheimer, G., & Wehrhahn, C. (1994). Discrimination of direction of motion in human vision. *Journal of Neurophysiology, 71,* 33–37.